Alz-QNet: A Quantum Regression Network for Studying Alzheimer's Gene Interactions

Debanjan Konar[1], Neerav Sreekumar[2], Richard Jiang[3], and Vaneet Aggarwal[1]
[1] *Purdue University, USA;* [2] *Indian Institute of Technology Tirupati, India;* [3] *Lancaster University, UK*

Understanding the molecular level mechanisms underpinning Alzheimer's disease (AD) by studying crucial genes associated with the disease remains a challenge. Alzheimer's, being a multifactorial disease, requires understanding the gene-gene interactions underlying it for theranostics and progress. In this article, a novel attempt has been made using a quantum regression to decode how some crucial genes in the AD Amyloid Beta Precursor Protein (APP), Sterol regulatory element binding transcription factor 14 ($FGF14$), Yin Yang 1 ($YY1$), and Phospholipase D Family Member 3 ($PLD3$) etc. become influenced by other prominent switching genes during disease progression, which may help in gene expression-based therapy for AD. Our proposed Quantum Regression Network (Alz-QNet)[a] introduces a pioneering approach with insights from the state-of-the art Quantum Gene Regulatory Networks (QGRN) to unravel the gene interactions involved in AD pathology, particularly within the Entorhinal Cortex (EC), where early pathological changes occur. Using the proposed Alz-QNet framework, we explore the interactions between key genes (APP, $FGF14$, $YY1$, $EGR1$, $GAS7$, $AKT3$, $SREBF2$, and $PLD3$) within the CE microenvironment of AD patients, studying genetic samples from the database $GSE138852$, all of which are believed to play a crucial role in the progression of AD. Our investigation uncovers intricate gene-gene interactions, shedding light on the potential regulatory mechanisms that underlie the pathogenesis of AD, which helps us to find potential gene inhibitors or regulators for theranostics.

I. INTRODUCTION

Alzheimer's disease (AD) presents a formidable challenge in healthcare, characterized by progressive cognitive decline and neurodegeneration [1]. The accumulation of peptides of Amyloid Beta ($A\beta$) from APP is a crucial factor in the pathology of AD [2]. Despite extensive research efforts over decades, the intricate mechanisms underlying AD remain elusive, impeding the development of effective therapeutic interventions [3]. The hypothesis of the amyloid cascade, which attributes neurotoxicity and neuronal loss to the accumulation of $A\beta$ peptides, has been a prominent theory but has faced limitations in translating it into successful treatments [4]. Clinical trials targeting $A\beta$ accumulation have produced disappointing results, underscoring the multi-factorial nature of AD pathogenesis influenced by factors such as Reactive Oxygen Species (ROS) and ferroptosis [5]. Mounting evidence suggests that $A\beta$ deposition may be a downstream consequence rather than the primary driver of neurodegeneration, necessitating a reevaluation of therapeutic strategies and a deeper understanding of the molecular underpinnings of AD. The failure of the Amyloid Cascade hypothesis proved why AD is a multifactorial disease by debunking the myth that the gene that causes upregulation of amyloid beta, APP, is the primary driver of AD progression. Thus, the requirement to study a multigene model in the EC environment for potential gene control-based therapy has great potential.

Gene Regulatory Networks (GRN) [6, 7] are complex systems that govern gene expression and cellular processes. Understanding the dynamics of GRN is essential to elucidate the molecular mechanisms underlying physiological functions and disease states. In AD, the entorhinal cortex is particularly significant due to its early involvement in disease progression [8]. However, deciphering AD-related GRN presents challenges, which require innovative computational approaches to integrate multi-omics data and reveal the regulatory landscape of AD-associated genes [9]. Correlation- and regression-based methods are commonly employed techniques for GRN inference because of their computational efficiency. These methods typically compute correlation or regression coefficients for gene pairs based on the total number of cells in the dataset. However, they have limitations, as they treat gene pairs independently, failing to fully capture complex expression patterns by incorporating additional layers of information.

Quantum Computing (QC) harnesses the principles of quantum mechanics to perform computations beyond the capabilities of classical computers [10]. Unlike classical bits, which can only exist in a state of either 0 or 1, quantum bits or qubits can exist in superpositions of these states, enabling exponentially greater computational capacity and effective computations [11]. This exponential scaling opens avenues for solving computationally intractable problems in genomics [12]. For example, the human genome is given by 3 billion base pairs, which can be represented by 10^{10} classical bits, which are equivalent to 34 qubits (2^n possible states for each). Building upon the foundations of Quantum Machine Learning (QML) seeks to leverage quantum algorithms and hardware to enhance traditional machine learning techniques [13]. QML offers the promise of accelerated learning and improved performance in large datasets by exploiting quantum parallelism and entanglement [14]. Moreover, QML can poten-

[a] The Pytorch code for our Alz-QNet implementation is available at `https://anonymous.4open.science/r/QuantumGRN-E255`.

tially address challenges such as feature selection, dimensionality reduction, and pattern recognition, extending the applicability of machine learning to complex scientific domains [12, 13, 15, 16].
However, the main problem lies in the computational expense and complexity of quantum circuits, considering the costs of gates like controlled rotation, which are extensively used in QML (regression) circuits, which do not entirely make quantum computing an economically feasible option for data science in the short term [17]. The traditional method of Quantum Gene Regulatory Networks (QGRN) [18] suffers from being computationally very expensive to implement, as the quantum circuit with n qubits requires $n(n-1)$ controlled rotation gates and n rotation gates.
Recognizing these limitations, our Alz-QNet model harnesses the computational power of QML to explore high-dimensional genomic data to reveal intricate gene-gene interactions that contribute to the pathogenesis of AD [19]. In the midst of the intricate molecular mechanisms and unresolved queries in AD research, the integration of QML and GRN analysis holds promise to unravel the complexities of AD pathogenesis. Using quantum regression networks (Alz-QNet) inspired by GRN, the objective is to uncover the regulatory dynamics controlling key genes associated with AD, such as APP, $SREBF2$, and $EGR1$. Through this interdisciplinary effort, the aim is to advance the understanding of AD pathogenesis and lay the foundation for innovative therapeutic interventions targeting dysregulated gene networks [20].
The primary contributions of our work are summarized in the following.

1. In this study, we optimized Quantum Gene Regulatory Networks (QGRN) [18] to address the computational complexity and expense associated with the construction of variational quantum circuits for larger datasets. Our proposed Alz-QNet requires $\frac{n(n-1)}{2}$ controlled rotation gates over $n(n-1)$ for the QGRN model, demonstrating that a single controlled rotation gate between 2 qubits is sufficient to measure the interaction.

2. In our Alz-QNet circuit, the reduction of C_{R_Y} gates by half compared to the traditional QGRN [18], optimizes the number of variational parameters, $\theta_{x,y}$ between two qubits x and y. We observed that the value of $\theta_{x,y} = \theta_{y,x}$. It enhances the scalability potential of our proposed Alz-QNet.

3. The study also aimed to uncover how APP interacts with other key genes in AD, potentially offering information on control-based therapies for the gene expression of the disease.

4. Furthermore, beyond APP, the research used single nucleus RNA sequencing of the entorhinal cortex to explore less explored genes such as $YY1$, $SREBF2$, $PLD3$, $GAS7$, and $EGR1$.

Motivation: QML research in general has demonstrated better performance in term of generalization, expressivity, privacy and robustness [15, 16, 21]. It presents several notable advantages over the classical GRN reconstruction methods [18]. The QML algorithms utilized in GRN research leverage quantum superposition and entanglement, which allows them to capture complex, non-linear relationships between genes that classical algorithms may overlook. Furthermore, QML is better equipped to address the curse of dimensionality, which is especially pertinent given the high-dimensional nature of genomic data.

II. VARIOUS GENE TYPES WITH ALZHEIMER'S DISEASES

Comprehending the regulatory connections among pivotal genes associated with AD, such as APP, $SREBF2$, and other relevant genes, is essential for deciphering the molecular mechanisms driving AD pathogenesis. These genes are fundamental in synaptic function, lipid metabolism, and neuronal viability, and their dysregulation is associated with AD-related neuropathological processes, including $A\beta$ accumulation, tau hyperphosphorylation, and synaptic dysfunction [22].
At the forefront of AD research lies the APP, a gene pivotal to the disease's pathogenesis. Anomalies in APP processing lead to the generation of amyloid beta peptides, whose accumulation forms insoluble plaques - a hallmark of AD pathology [8, 23]. This neurotoxic cascade disrupts synaptic function, induces oxidative stress, and triggers inflammatory responses, ultimately resulting in synaptic dysfunction and neuronal loss. Continuing investigations actively explore strategies to modulate APP metabolism, prevent $A\beta42$ aggregation, or improve $A\beta42$ clearance as potential therapeutic interventions for AD [24].
However, APP is one component of the intricate puzzle of AD. Other genes, such as $AKT3$, $SREBF2$, $YY1$, $GAS7$, $EGR1$, $FGF14$, and $PLD3$, also play crucial roles in the pathogenesis of AD. For example, dysregulation of $AKT3$ signaling has been associated with insulin resistance, a common feature of AD pathology that exacerbates neurodegeneration. Studies suggest that activated $AKT3$ promotes neuronal survival by inhibiting Glycogen Synthase Kinase-3 β ($GSK-3\beta$), a pro-apoptotic protein, and enhances adult neurogenesis in neural stem cells (NSC). Conversely, dysregulated $AKT3$ signaling may worsen neuronal vulnerability and contribute to AD pathogenesis, particularly in conditions like insulin resistance [25]. Therefore, exploring the molecular mechanisms underlying $AKT3$ dysregulation in AD provides valuable information on potential therapeutic targets to mitigate neurodegeneration and cognitive decline in individuals with AD [26, 27].
$SREBF2$, a key regulator of lipid metabolism, interacts with pathways involving crucial genes in AD, impact-

ing processes such as amyloid-beta production, transcriptional regulation, and insulin signaling. Dysregulation of $SREBF2$ signaling is associated with neurodegeneration, exacerbating amyloid beta accumulation, synaptotoxicity, and memory deficits in neuronal cells [28]. Furthermore, disrupted $SREBF2$ signaling affects cholesterol homeostasis in brains with AD, preventing the clearance of plaques $A\beta$ and increasing oxidative stress in neuronal cells. Recent research has highlighted the role of $SREBF2$ in AD, demonstrating significant changes in its nuclear translocation and activation patterns in AD brains and relevant animal models. Specifically, reduced nuclear translocation of mature $SREBF2$ ($mSREBP2$) is observed in AD brains, with tau modifications associated with these alterations [2, 29].

The involvement of $YY1$ in regulating the Fuz gene adds another layer of significance to its role in AD research. Aberrant $YY1$ activity can result in excessive methylation of the Fuz gene promoter, leading to reduced transcription. This alteration affects the polarity of the planar cells and subsequent cell stability, which are crucial for neuronal health. The elevated Fuz transcript levels observed in individuals with AD pathology suggest that $YY1$-mediated modifications of the Fuz gene may contribute to neuronal apoptosis and neurodegeneration in AD. Thus, unraveling the interplay between $YY1$ and the Fuz gene provides information on additional mechanisms underlying AD pathogenesis, offering potential avenues for therapeutic intervention targeting $YY1 - Fuz$ interactions to mitigate neuronal loss and cognitive decline in AD. Targeting $YY1$ expression or activity could hold therapeutic potential for alleviating AD pathology, making it a significant focus in the pursuit of effective AD treatments [4, 30].

$GAS7$, $EGR1$, $FGF14$, and $PLD3$ each play distinct roles in AD pathogenesis, influencing processes such as tau phosphorylation, synaptic plasticity, and lipid metabolism. Dysregulated expression of $GAS7$ in neurons has been associated with altered microtubule transport proteins, potentially leading to tau dysregulation and increased susceptibility to AD development. Recent research has shed light on the involvement of $GAS7$ in neuronal maturation and morphogenesis, further implicating its role in the progression of AD [31]. $GAS7$ expression promotes the formation of dendrite-like processes and filopodia projections in neuronal cells, enhancing neurite outgrowth and microtubule bundling. These findings suggest that $GAS7$ governs neural cell morphogenesis by coordinating actin filaments and microtubules, thereby influencing neuronal maturation and potentially impacting AD progression. The intricate interplay among these genes unveils a complex network of molecular events driving AD progression [32]. $EGR1$'s modulation of acetylcholinesterase mRNA and protein levels indicates its significant contribution to alterations in acetylcholine signaling observed in AD, where acetylcholine depletion is prominent. Furthermore, $EGR1$'s regulation of $miRNA{-}132$, impacting the nucleus basalis of Meynert rich in acetylcholine, underscores its role in AD-related neurotransmitter dysregulation [33]. Recent studies have provided promising information on the therapeutic potential of $EGR1$ in AD. Silencing $EGR1$ in AD mouse models reduces tau phosphorylation, decreases amyloid-beta pathology, and improves cognition [34].

$EGR1$ regulates tau phosphorylation and amyloid synthesis by influencing the activities of $Cdk5$ and $BACE-1$, respectively, suggesting its potential as a therapeutic candidate for the treatment of AD [35]. Conversely, dysfunction in sodium channel signaling due to $FGF14$ deficiency has been linked to neurological disorders, such as schizophrenia [36]. In particular, modulation of sodium channel signaling $FGF14$' can affect amyloid beta pathology, with $PPAR-\gamma$ agonists showing promise by phosphorylating $FGF14$ and modulating sodium channel signaling. This suggests a potential role for $FGF14$ as a therapeutic target in the management of neuronal dysfunction and memory loss observed in early AD. Additionally, $FGF14$ demonstrates neuroprotective effects by inhibiting $MAPK$ signaling, highlighting its potential as a therapeutic agent for neurodegenerative conditions. Its complex interactions with voltage-gated sodium channels at the axonal initial segment influence neuronal excitability, synaptic transmission, and neurogenesis, affecting cognitive and affective behavioral outcomes [37]. In translational studies, $FGF14$ has been increasingly associated with diseases related to cognitive and affective domains, including neurodegeneration, indicating its involvement as a converging node in the etiology of complex brain disorders, further emphasizing its potential significance in AD pathogenesis [38].

$PLD3$'s involvement in the formation of amyloid plaque-associated axonal spheroids highlights its role in the dysfunction of the neural network in AD [39]. Mechanically, $PLD3$ encodes a highly concentrated lysosomal protein in axonal spheroids, with its overexpression leading to spheroid enlargement and exacerbated axonal conduction blockades. In contrast, deletion of $PLD3$ reduces the size of the spheroid and improves the function of the neural network. Targeted modulation of endolysosomal biogenesis mediated by $PLD3$ in neurons presents a promising avenue to reverse axonal spheroid-induced neural circuit abnormalities in AD, independent of amyloid removal. In AD brains, suppressing inappropriate PLD signaling has shown the potential to enhance synaptic resilience and decelerate cognitive decline, offering therapeutic advantages in AD management [40].

Studying the gene regulation of all eight genes collectively provides a comprehensive understanding of AD pathophysiology. By elucidating the dynamic interactions among these genes, researchers can uncover common underlying mechanisms and novel therapeutic targets for AD [40].

A. Single-Nucleus RNA Sequencing

Single-nucleus RNA sequencing ($snRNA-seq$) is a powerful technique to analyze gene expression patterns at the single-cell level. Unlike traditional RNA sequencing methods, which require intact cells, $snRNA-seq$ enables analysis of gene expression of individual nuclei extracted from tissues, including complex tissues such as the brain [41]. The snRNA-seq process involves several steps:

1. Nuclei Isolation: Tissue samples are dissociated to release individual nuclei while preserving RNA integrity.

2. Library Preparation: RNA is extracted from isolated nuclei, and cDNA libraries are generated by reverse transcription.

3. Sequencing: cDNA libraries are sequenced using high-throughput sequencing platforms, generating millions of short reads corresponding to RNA transcripts.

4. Data Analysis: Bioinformatics tools are used to align sequencing reads to a reference genome, quantify gene expression levels, and perform downstream analyzes, such as identifying cell types and characterizing gene regulatory networks.

5. Studying Gene Expression: $snRNA-seq$ provides information on gene expression heterogeneity within cell populations and allows researchers to identify rare cell types and transcriptomic changes associated with various biological processes and disease states. By profiling gene expression at the single-cell level, $snRNA-seq$ enables the discovery of novel cell types, regulatory pathways, and biomarkers with high resolution and sensitivity [42].

III. QUANTUM COMPUTING THEORY

A. Qubits and Basis States

In quantum computing, the basic unit is *qubit*. A qubit can exist in a superposition of the states $|0\rangle$ and $|1\rangle$, represented as [43]:

$$|\psi\rangle = \alpha|0\rangle + \beta|1\rangle\,, \tag{1}$$

where α and β are complex numbers such that $|\alpha|^2 + |\beta|^2 = 1$. The states $|0\rangle$ and $|1\rangle$ are the computational basis states.

B. Quantum Gates

Quantum gates manipulate qubits through unitary operations. Here are some basic quantum gates and their operations [43]:

1. NOT Gate: The NOT (X) gate flips the state of a qubit as follows [44]:

$$X = \begin{pmatrix} 0 & 1 \\ 1 & 0 \end{pmatrix}, \tag{2}$$

$$X|0\rangle = |1\rangle, \quad X|1\rangle = |0\rangle\ . \tag{3}$$

2. Hadamard Gate: The Hadamard (H) gate creates a superposition of the states $|0\rangle$ and $|1\rangle$ [44]:

$$H = \frac{1}{\sqrt{2}} \begin{pmatrix} 1 & 1 \\ 1 & -1 \end{pmatrix}, \tag{4}$$

$$H|0\rangle = \frac{1}{\sqrt{2}}(|0\rangle + |1\rangle), \quad H|1\rangle = \frac{1}{\sqrt{2}}(|0\rangle - |1\rangle)\ . \tag{5}$$

3 Controlled-NOT Gate: The Controlled-NOT (C_X) gate flips the target qubit if the control qubit is in the state $|1\rangle$ [44]:

$$C_X = \begin{pmatrix} 1 & 0 & 0 & 0 \\ 0 & 1 & 0 & 0 \\ 0 & 0 & 0 & 1 \\ 0 & 0 & 1 & 0 \end{pmatrix}\ . \tag{6}$$

The action of a C_X gate on the basis states:

$$C_X|00\rangle = |00\rangle, \quad C_X|01\rangle = |01\rangle\ . \tag{7}$$

$$C_X|10\rangle = |11\rangle, \quad C_X|11\rangle = |10\rangle\ . \tag{8}$$

4. Rotation Gate: The rotation gate around the Y-axis (R_Y) rotates the qubit state by an angle θ [44]:

$$R_Y(\theta) = \begin{pmatrix} \cos(\frac{\theta}{2}) & -\sin(\frac{\theta}{2}) \\ \sin(\frac{\theta}{2}) & \cos(\frac{\theta}{2}) \end{pmatrix}\ . \tag{9}$$

5. Controlled-R_Y Gate: The controlled-R_Y (C_{R_Y}) gate rotates around the Y-axis on the target qubit if the control qubit is in the state $|1\rangle$. This can be constructed using a C_X gate and R_Y gates as follows [44]:

$$C_{R_Y}(\theta) = \begin{pmatrix} 1 & 0 & 0 & 0 \\ 0 & 1 & 0 & 0 \\ 0 & 0 & \cos(\frac{\theta}{2}) & -\sin(\frac{\theta}{2}) \\ 0 & 0 & \sin(\frac{\theta}{2}) & \cos(\frac{\theta}{2}) \end{pmatrix}\ . \tag{10}$$

This operation can be decomposed into a sequence involving a C_X gate and $R_Y$gates:

$$C_{R_Y}(\theta) = (I \otimes R_Y(\frac{\theta}{2})) \cdot C_X \cdot (I \otimes R_Y(-\frac{\theta}{2})) \cdot C_X\ . \tag{11}$$

Here, I is the identity matrix. The standard basis state table for controlled rotation gates is provided in Table I

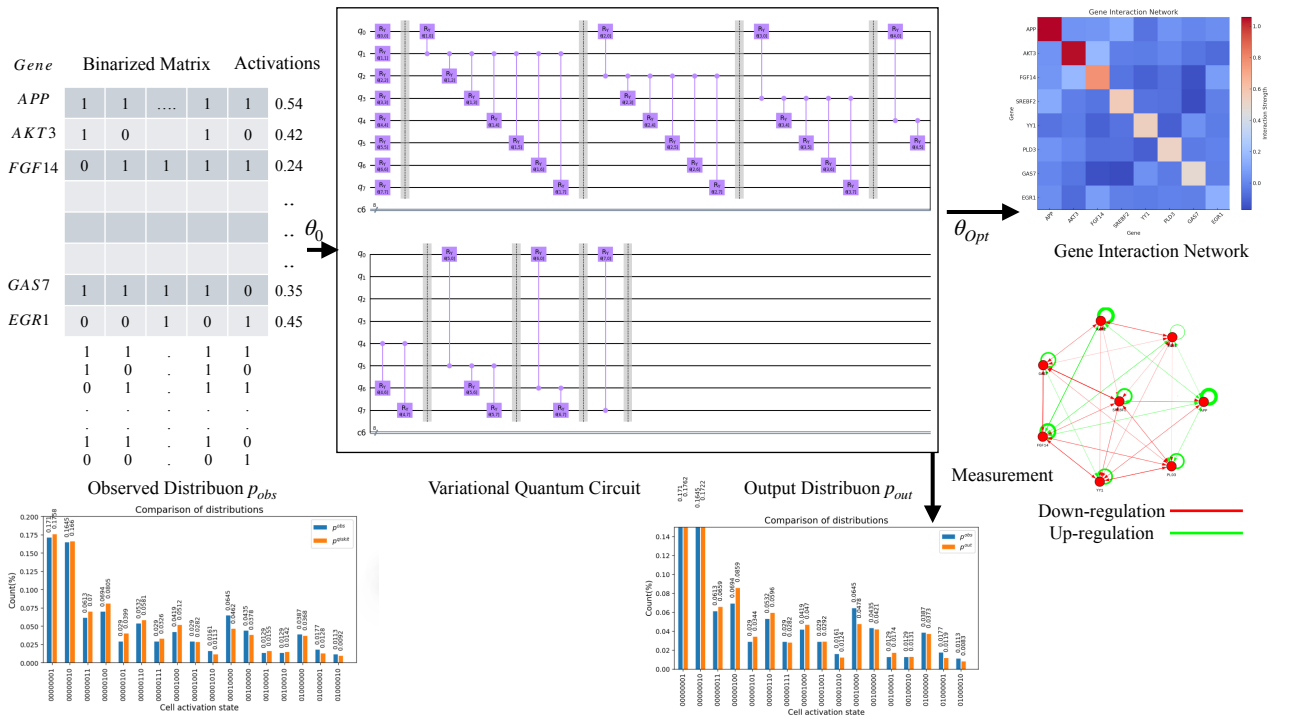

FIG. 1: A Quantum Regression Network (Alz-QNet) relying on Variational Quantum Circuit (VQC) to study Alzheimer's gene interactions (The circuit is continued from top to bottom).

Basis state $\|x\rangle$	$C_{R_Y}(\theta)\|x\rangle$
$\|00\rangle$	$\|00\rangle$
$\|01\rangle$	$\|01\rangle$
$\|10\rangle$	$\cos\left(\frac{\theta}{2}\right)\|10\rangle + \sin\left(\frac{\theta}{2}\right)\|11\rangle$
$\|11\rangle$	$-\sin\left(\frac{\theta}{2}\right)\|10\rangle + \cos\left(\frac{\theta}{2}\right)\|11\rangle$

TABLE I: Mapping basis states using a $C_{R_Y}(\theta)$ gate.

IV. QUANTUM REGRESSION NETWORK ARCHITECTURE

The proposed Alz-QNet model centered on studying the 8 genes specific to Alzheimer's disease by significantly reducing the cost of the C_{R_Y} gates through a bypass mechanism, thereby decreasing their number by half to analyze Gene Regulatory Networks (GRN) [6] with reduced computational complexity. Inspired by the Quantum Gene Regulatory Networks (QGRN) [18], our proposed Alz-QNet, as shown in Fig. 1, leverages the quantum entanglement quantum computing offers to explore gene regulatory relationships. In the proposed Alz-QNet model, each qubit represents a gene and initializes to phase 0. The Alz-QNet is structured into two sections: the encoder and regulation layers. The encoder layer translates $snRNA - seq$ data into a superposition state, while the regulation layers entangle qubits to model gene-gene interactions within the quantum framework. Through these layers, we construct an 8×8 matrix, with an initial unknown value of $\theta_{x,y}$ in the C_{R_Y} gates entangling 2 qubits, where x represents the control qubit (gene) and y represents the target qubit (gene). The optimized values of each θ in the matrix correspond to the strength of gene interaction. Traditional Laplace smoothing and the gradient descent algorithm are used for the optimization process to minimize a loss function based on Kullback-Leibler (KL) divergence [45].

Our Alz-QNet model utilizes a C_{R_Y} gate to establish connections between each pair of qubits in the regulation layers, simulating the regulatory relationships between two genes. The rotation angle of the C_{R_Y} gate signifies the strength of the interaction between the control gene and the target gene. Following optimization, these rotation angles are parameterized and translated into the adjacency matrix to construct a GRN. A primary unit circuit is depicted in Fig. 3, initialized in the $|00\rangle$ state. This circuit comprises a control qubit (1^{st} qubit, rotated with a R_Y gate at an angle ϕ_1), a target qubit (2^{nd} qubit, rotated with a R_Y gate at an angle ϕ_2) and a C_{R_Y} gate with a rotation angle θ.

We measured the output register to obtain the output distribution p_{out} of the basis states. The probability of a particular state in p_{out} was set to 0, and the remaining distribution was rescaled to sum to 1. Laplace smoothing was applied to reshape p_{obs} and p_{out} into smoothed distributions $\tilde{p}_{\text{obs}}$ and $\tilde{p}_{out}$, respectively. These smoothed distributions are computed as follows:

$$\tilde{p}(x) = \frac{p(x) + \alpha}{N + \alpha \cdot |X|}, \tag{12}$$

where α is the smoothing parameter (typically set to 1), N is the total number of occurrences in the distribution, and $|X\rangle$ is the size of the distribution's support. In other words, $\tilde{p}$ represents the original distribution after smoothing.

A. Loss Function

The loss function, comprising the KL divergence ($\mathcal{L}_{KL}$) [45] and a constraint term ($\mathcal{L}_c$), is defined as follows:

$$\mathcal{L}_{KL} = \sum p_{obs} \log \frac{p_{obs}}{p_{out}} \,. \tag{13}$$

$$\mathcal{L}_c = \sum (\theta - \theta_0)^2 \,, \tag{14}$$

where θ is the parameter in the proposed Alz-QNet model and θ_0 is the initial parameter set. Thus, the total loss function was defined as:

$$\mathcal{L} = \mathcal{L}_{KL} + \lambda \mathcal{L}_c \,, \tag{15}$$

where λ is a dynamic coefficient that rescales $\mathcal{L}_c$ to the same order of magnitude as $\mathcal{L}_{KL}$. In summary, the term $\mathcal{L}_{KL}$ aligns the output distribution p_{out} with the observed distribution p_{obs}, while the term $\mathcal{L}_c$ prevents any parameter θ from deviating significantly from θ_0.
Optimization has been performed by iteratively minimizing the loss function until it has reached a threshold value of $2^n \times 10^{-4}$ using a modified gradient descent algorithm with a learning rate (η) of 0.05. If this threshold is unmet, optimization has continued for a predefined number of iterations ι. The parameter θ in iteration ι was updated as:

$$\theta^{(\iota+1)} = \theta^{(\iota)} - \eta \nabla \mathcal{L}^T \,, \tag{16}$$

where $\nabla\mathcal{L}$ is the gradient of the loss function, ensuring θ remains a symmetric matrix. In the proposed Alz-QNet, $\theta_{k,k}$ as the parameter for the R_Y gate on the k^{th} qubit in the L_e layer, and $\theta_{k,p}$ for the C_{R_Y}, n gate with the k^{th} qubit as control and the p^{th} qubit as target in the L_k layer of an n-qubit system. For our case where $n = 8$, the layers are defined as follows:

$$L_e = R_Y(\theta_{7,7}) \otimes R_Y(\theta_{6,6}) \otimes \cdots \otimes R_Y(\theta_{1,1}) \otimes R_Y(\theta_{0,0}) \,, \tag{17}$$

and

$$\begin{aligned} L_k = \prod_{i=0, i\neq k}^{7} C_{R_Y}, n(\theta_{k,i}) = C_{R_Y}, n(\theta_{k,7}) \\ \otimes \cdots \otimes c - R_Y, n(\theta_{k,1}) \otimes C_{R_Y}, n(\theta_{k,0}) \,. \end{aligned} \tag{18}$$

In our Alz-QNet circuit, we have reduced the number of C_{R_Y} gates by half compared to the traditional QGRN [18], optimizing the upper triangular matrix of $\theta_{x,y}$. We observed that the value of $\theta_{a,b} = \theta_{b,a}$, demonstrating that a single controlled rotation gate between 2 qubits is sufficient to measure the interaction. By manually setting $\theta_{a,b} = \theta_{b,a}$, we construct the entire matrix:

$$\theta = \begin{pmatrix} \theta_{0,0} & \theta_{0,1} & \cdots & \theta_{0,7} \\ \theta_{1,0} & \theta_{1,1} & \cdots & \theta_{1,7} \\ \vdots & \vdots & \ddots & \vdots \\ \theta_{7,0} & \theta_{7,1} & \cdots & \theta_{7,7} \end{pmatrix} \,. \tag{19}$$

In the modified constraint loss L_c, the parameter θ_0 represents the initial rotation angles of the quantum gates, reflecting prior assumptions or biological priors. In our implementation, θ_0 is initialized to 0 for all non diagonal elements in the matrix, thus having 0 bias. All diagonal elements are having θ_0 of $2\arcsin(\sqrt{a_k})$, where a_k is the activation ratio for the k^{th} gene.

V. SIMULATIONS

Our work is integrated with Qiskit, an open-source quantum computing library that simulates a noisy quantum circuit using the Aer Simulator backend with default parameters.

A. Dataset Processing and Parameter Initialization

The dataset GSE138852 [42] comprises single-nucleus RNA sequencing (snRNA-seq), and has been used to analyze the Entorhinal Cortex (EC) tissues derived from the control and Alzheimer's Disease (AD) brains of twelve individuals. This approach resulted in the identification of a total of 13, 214 high-quality nuclei, all of which are sourced from AD-positive patients and we used the initial subset of 1, 041 cells.
Initially, the data set with A genes and B cells is normalized using Pearson's residual method. Subsequently, attention was directed to the chosen 8 genes. The normalized expression matrix X has been binarized by applying a threshold of 0, resulting in a binarized matrix X_b. In this binarization process, the expression values above 0 are set to 1, while the values equal to or below 0 are set to 0. The binarized matrix X_b has dimensions of $8 \times m$. Labels are assigned by creating string vectors based on binarized expression values of selected genes 8 for each cell, representing the activation states of the cells. To compute the observed distribution p_{obs}, we calculated the percentage of the occurrence of each label among m cells. In p_{obs}, the percentage for the label ℓ was set to 0, and the remaining distribution was rescaled to the sum of 1. This approach ensures that only cells that express at least one of the n genes are considered informative, addressing the lack of consistency inherent in the $snRNA - seq$ data due to dropout events during sequencing. The non-diagonal elements associated with C_{R_Y} gates were initialized to 0. In contrast, the diagonal

elements corresponding to the R_Y gates are initialized using $\theta = 2\arcsin(\sqrt{a_k})$, where a_k is the activation ratio for the k^{th} gene. This initialization ensures that for each qubit, the probability of measuring a state of 1 aligns with the activation ratio of the respective gene after the L_e layer [18].

B. Simulation Results

In our investigation, we used $snRNA-seq$ EC data from AD patients to explore the genetic and molecular mechanisms underlying this neurodegenerative disorder ($GSE138852$). The EC crucial for memory and navigation is among the primary regions impacted by AD, making it an ideal focus for studying early pathological changes. From this dataset, we selected 8 specific genes: APP, $SREBF2$, $GAS7$, $PLD3$, $YY1$, $FGF14$, $AKT3$, and $EGR1$. In quantum simulations, a nodal graph is generated using Qiskit along with the observed vs. output frequency distribution graph and the observed vs. simulated frequency distribution graph, as shown in Fig. 2, which resembles the classical GRN [7]. In addition, we also simulated the QGRN as a baseline model and found that it produced a similar probability distribution to Alz-QNet, as illustrated in Fig. 3, while saving computations.

$$\begin{bmatrix}
1.058 & 0.044 & 0.050 & 0.123 & -0.054 & 0.044 & -0.000 & 0.025 \\
0.044 & 1.044 & 0.174 & -0.022 & -0.025 & 0.002 & -0.047 & -0.078 \\
0.050 & 0.174 & 0.773 & -0.050 & -0.105 & -0.066 & -0.153 & 0.074 \\
0.123 & -0.022 & -0.050 & 0.562 & -0.058 & -0.060 & -0.168 & -0.019 \\
-0.054 & -0.025 & -0.105 & -0.058 & 0.540 & -0.112 & 0.034 & -0.029 \\
0.044 & 0.002 & -0.066 & -0.060 & -0.112 & 0.524 & -0.033 & -0.011 \\
-0.000 & -0.047 & -0.153 & -0.168 & 0.034 & -0.033 & 0.485 & -0.019 \\
0.025 & -0.078 & 0.074 & -0.019 & -0.029 & -0.011 & -0.019 & 0.138
\end{bmatrix}$$

The above matrix shows the $\theta_{x,y}$ values, where each row and column corresponds to a different gene. The black upper triangular matrix is the optimized value of theta obtained, and the lower triangular matrix was constructed from the equal values of $\theta_{x,y} = \theta_{y,x}$.
The red lines show the down-regulated networks, and the green lines show the up-regulated networks. Our graph model delves deeper into the genetic interactions of an AD patient's brain taken from the EC. In addition to the gene interactions that affect prominent genes like APP and $AKT3$, which have direct correlations, our findings extend and support the detailed epigenetic and transcriptomic insights [1], particularly through the interactions involving $YY1$ and $PLD3$, as shown in Fig. 2.

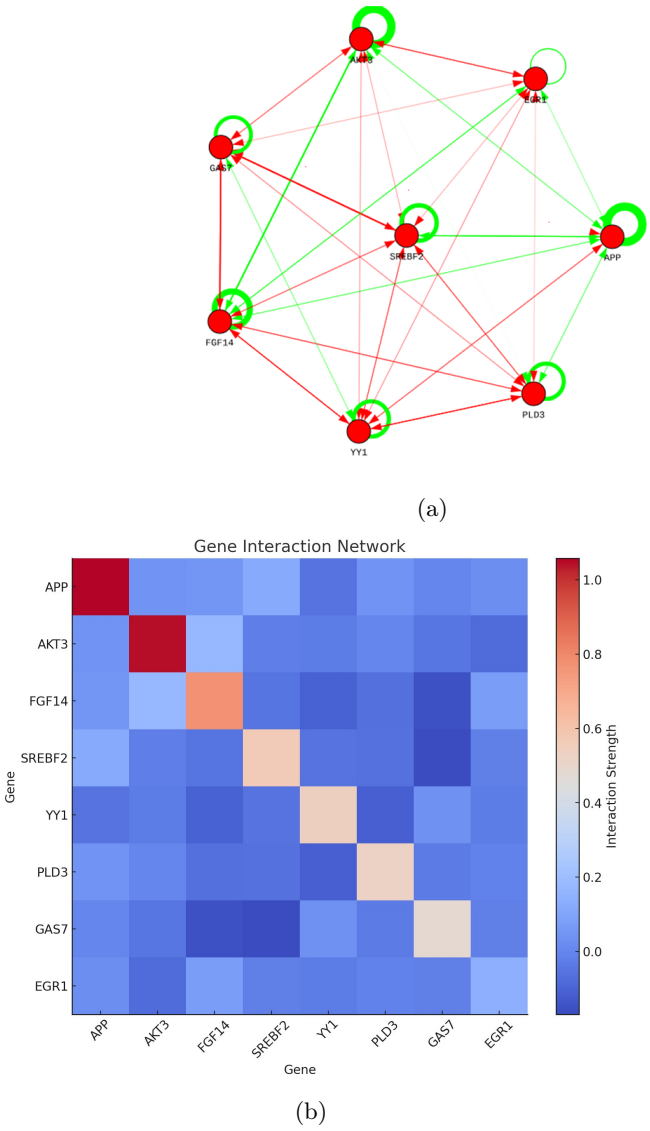

FIG. 2: (a) The nodal graph, where each node corresponds to the specific gene and the edges determine the gene regulatory interactions. Green edges represent upregulation, and red edges represent downregulation. The weight of the edges determines the strength of the interaction between genes. (b) Heat map generated to study Alzheimer's gene interactions for our model and quantify graph results.

Fig. 4 illustrates the impact of rotation angles θ and ϕ_1 on the amplitude $|\mu|^2$ of the $|1\rangle$ state in a quantum circuit. Each heatmap corresponds to a different fixed value of ϕ_1 $(0, 0.25\pi, 0.5\pi, 0.75\pi)$, while θ (X-axis) and ϕ_1 (Y-axis) vary continuously.The heatmaps reveal symmetric patterns across the parameter space. This symmetry, stemming from the property $\theta_{x,y} = \theta_{y,x}$ allows us to encode the same amplitude information with half the number of gates. For example, the heatmap values for (ϕ_1, θ) and (ϕ_2, θ) by fixing either and varying the other and observing the symmetry in the heatmap to conclude that they overlap significantly, demonstrating that redundant gates contribute no additional unique information. The regions of high and low amplitude values are nearly invariant to the interchanging of ϕ_1 and ϕ_2, further validating the symmetric property of the C_{R_Y} gates. Certain boundary conditions (e.g., $\phi_1 = 0$ or $\phi_1 = \pi$) exhibit near-linear dependence of amplitudes, simplifying the overall amplitude structure. Leveraging these symmetric properties, we reduce the number of C_{R_Y} gates by 50% without al-

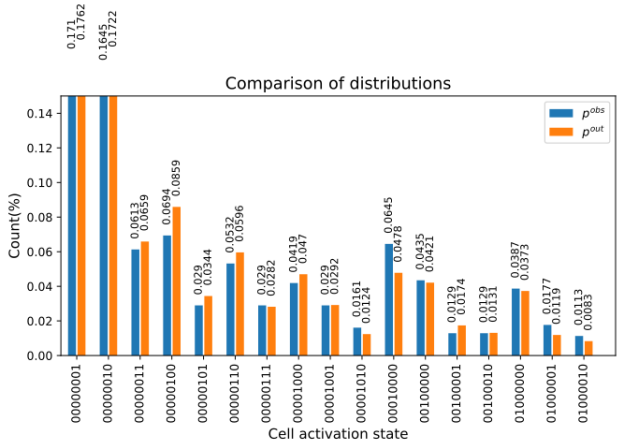

(a)

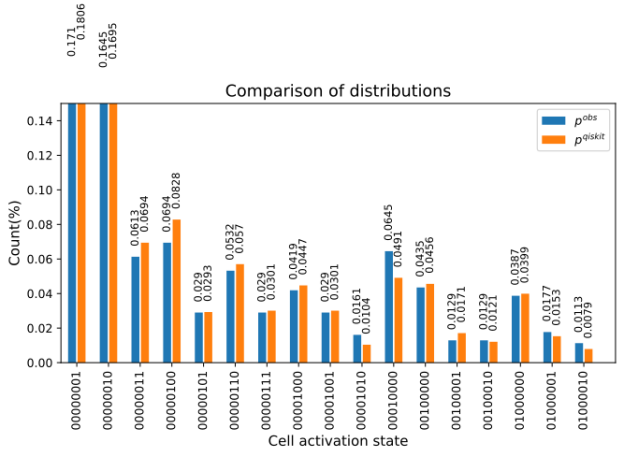

(b)

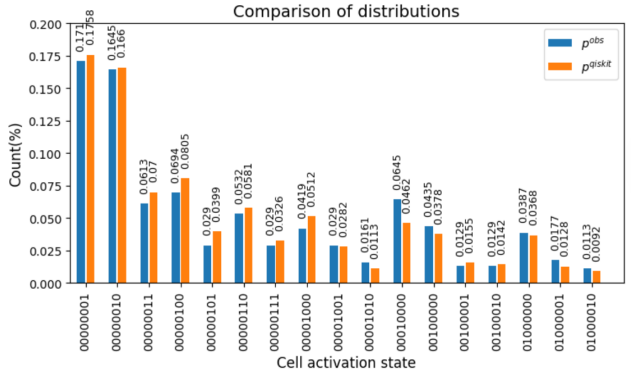

(c)

FIG. 3: (a) The observed vs output frequency distributions graph for Alz-QNet, (b) The observed vs simulated frequency distributions graph for Alz-QNet, and (c) The observed vs simulated frequency distributions graph for QGRN.

tering the final quantum state representation. This reduction directly translates to lower computational cost and complexity, particularly for large QGRN networks with multiple gene-gene interactions.

VI. DISCUSSIONS

In this article, integrating transcriptomic and epigenetic data, our Alz-QNet offers insights into how regulatory mechanisms at the genetic and epigenetic levels contribute to AD. This supports the study conducted by Grubman *et al.* [1] with an emphasis on considering transcriptional and epigenetic factors to understand brain function and disease, highlighting the importance of integrating multiple layers of biological data to understand the molecular foundations of diseases like Alzheimer's. This interdisciplinary methodology offers valuable insight into the molecular foundations of AD and underscores the promising role of QML research in elucidating complex biological phenomena.

A. $YY1$ and $PLD3$ Interaction

$YY1$ is a transcription factor with dual gene activation and repression roles. It influences gene expression epigenetically by recruiting proteins that modify chromatin structure. Our results show a negative interaction between $YY1$ and $PLD3$ (-0.112907), suggesting $YY1$'s repressive role on $PLD3$. This aligns with the known function of $YY1$ in gene repression and epigenetic regulation.

B. Role of $PLD3$ in AD

$PLD3$ is involved in processing APP and regulating amyloid-beta levels, which are critical in AD pathology. Our study reveals complex interactions between $PLD3$ and other genes, such as APP and $SREBF2$. These interactions suggest that the regulatory network of $PLD3$ is influenced by both transcriptional and epigenetic mechanisms, supporting the emphasis of the neurobiology literature on the importance of epigenetic modifications in brain development and disease.

C. Integration of Epigenetic and Transcriptomic Data

The work of Grubman *et al.* [1] provides a comprehensive map of gene expression and epigenetic modifications, allowing the identification of key regulatory genes. Our study extends these findings by focusing on the entorhinal cortex in AD, demonstrating how specific gene-gene interactions are modulated by transcriptic factors. The interactions involving $YY1$ and $PLD3$ in our network analysis reflect that the complex regulatory dynamics are driven by changes in gene expression, rather than direct epigenetic modifications. We highlight the importance of these regulatory interactions within the context of gene expression, acknowledging the broader potential for future research to explore epigenetic mechanisms to study

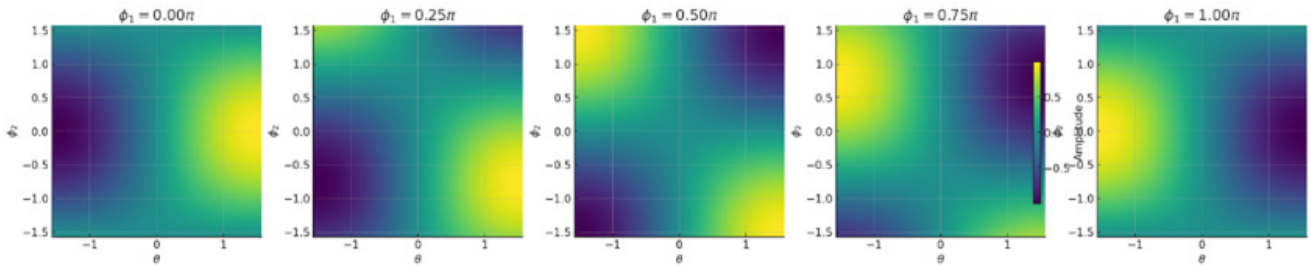

FIG. 4: Illustrates the impact of rotation angles θ and ϕ_1 on the amplitude $|\mu|^2$ of the $|1\rangle$ state in a quantum circuit. Each heatmap corresponds to a different fixed value of ϕ_1 $(0, 0.25\pi, 0.5\pi, 0.75\pi)$, while θ (X-axis) and ϕ_1 (Y-axis) vary continuously. The colour intensity represents the amplitude magnitude of the target qubit's $|1\rangle$ state, with brighter regions indicating higher amplitudes.

molecular mechanisms underpinning the gene regulatory activity in future.

VII. CONCLUSION

The current study proposes a novel approach that combines the principles of QML, and GRN analysis to investigate the complex gene-gene interactions involved in AD pathology within the EC. Our proposed Alz-QNet model has the potential for significantly enhanced computational power, enabling faster and more precise modeling of intricate gene interactions. This advancement can lead to a deeper understanding of biological processes and can offer groundbreaking insights into gene regulation and expression. Leveraging the precision of quantum computing could revolutionize personalized medicine by tailoring treatments to individual genetic profiles. Furthermore, quantum algorithms have the capability to optimize biological processes and provide efficient solutions to complex biological challenges, making them a potent tool for simulating and understanding intricate systems. Notably, we have reduced the computational cost by nearly half compared to traditional QGRN, providing a progressive edge in addressing the computational expense issue.

However, the current state of quantum computing is still in its nascent stages, with limited availability and challenges such as errors and decoherence. Modeling the GRN at the quantum level is highly complex and resource-intensive, necessitating specialized hardware, software, and expertise, which can be costly. Scalability poses a significant hurdle, as existing quantum computers struggle to handle the vast datasets typical of gene regulatory networks. Given the constraints of hardware qubits and noise, approximation techniques such as the utilization of tensor rings may offer a viable approach in the future for scaling up data input while ensuring accurate results.

VIII. DATA AVAILABILITY

The Alzheimer's dataset used for our model can be found at: `https://www.ncbi.nlm.nih.gov/geo/query/acc.cgi?acc=GSE138852`

IX. CODE AVAILABILITY

The Pytorch code for our Alz-QNet implementation is available in Qiskit simulations at `https://anonymous.4open.science/r/AD_Quantum-2BE8`.

[1] A. Grubman, G. Chew, J. F. F. Ouyang,*et al.*, "A single-cell atlas of entorhinal cortex from individuals with Alzheimer's disease reveals cell-type-specific gene expression regulation," *Nature Neuroscience*, vol. 22, 2019, doi: `https://doi.org/10.1038/s41593-019-0539-4`.

[2] C. Wang, F. Zhao, K. Shen, *et al.*, "The sterol regulatory element-binding protein 2 is dysregulated by tau alterations in Alzheimer disease," *Brain pathology*, vol. 29, no. 4, pp. 530–543, 2018, doi: `10.1111/bpa.12691`.

[3] J. Palop and L. Mucke, "Amyloid-β–induced neuronal dysfunction in Alzheimer's disease: from synapses toward neural networks," *Nature Neuroscience*, vol. 13, no. 7, pp. 812–818, 2010, doi: `https://doi.org/10.1038/nn.2583`.

[4] K. Nowak, C. Lange-Dohna, U. Zeitschel, *et al.*, "The transcription factor Yin Yang 1 is an activator of BACE1 expression," *Journal of Neurochemistry*, vol. 96, pp. 1696–1707, 2006, doi: `10.1111/j.1471-4159.2006.03692.x`.

[5] K. Vossel, M. Tartaglia, H. Nygaard, *et al.*, "Epileptic activity in Alzheimer's disease: causes and clinical relevance", *The Lancet Neurology*, vol. 16, no. 4, pp. 311–322, 2017, doi: `https://doi.org/10.1016/s1474-4422(17)30044-3`.

[6] G. Karlebach, and R. Shamir, "Modelling and analysis of gene regulatory networks," *Nat. Rev. Mol. Cell Biol.*, vol.

9, pp. 770–780, 2008, doi: https://doi.org/10.1038/nrm2503.

[7] E. Davidson and M. Levin, "Gene regulatory networks," *Proc. of the Nat. Acad. of Sc.*, vol. 102, no. 14, pp. 4935–4935. doi: https://doi.org/10.1073/pnas.0502024102.

[8] D. Selkoe and J. Hardy, "The amyloid hypothesis of alzheimer's disease at 25 years", *EMBO Molecular Medicine*, vol. 8, no. 6, p. 595–608, 2016, doi: https://doi.org/10.15252/emmm.201606210.

[9] G. W. van Hoesen, B. T. Hyman and A. R. Damasio, "Entorhinal cortex pathology in Alzheimer's disease," *Hippocampus*, vol. 1, pages 1-8, 1991, doi: https://doi.org//10.1002/hipo.450010102.

[10] L. Marchetti, R. Nifosì, P. L. Martelli, *et al.*, "Quantum computing algorithms: getting closer to critical problems in computational biology," *Briefings in Bioinf.*, vol. 23, no. 6, 2022, doi: 10.1093/bib/bbac437.

[11] D. Konar, S. Bhattacharyya, T. K. Gandhi, *et al.*, "3-D Quantum-Inspired Self-Supervised Tensor Network for Volumetric Segmentation of Medical Images," *IEEE Tran. on Neu. Net. and Learning Sys.*, pp 1-15, doi: 10.1109/TNNLS.2023.3240238.

[12] S. Pal, M. Bhattacharya, S. S. Lee, *et al.*, "Quantum Computing in the Next-Generation Computational Biology Landscape: From Protein Folding to Molecular Dynamics," *Science*, vol. 66, no. 2, pages 163–178, 2024, doi: 10.1007/s12033-023-00765-4.

[13] J. Biamonte, P. Wittek, S. Lloyd, et al., "Quantum Machine Learning," *Nature*, vol. 549, pp. 195–202, 2018, doi: https://doi.org/10.1038/nature23474.

[14] D. Konar, S. Bhattacharyya, B. K. Panigrahi, *et al.*, "Qutrit-Inspired Fully Self-Supervised Shallow Quantum Learning Network for Brain Tumor Segmentation," *IEEE Trans. on Neural Net. and Learning Sys.*, vol. 33, no. 11, pp. 6331–6345, Nov. 2022, doi: 10.1109/TNNLS.2021.3077188.

[15] D. Konar, E. Gelenbe, S. Bhandary, *et al.*, "Random Quantum Neural Networks for Noisy Image Recognition," *2023 IEEE Int. Conference on Quan. Comp. & Eng. (QCE)*, Bellevue, USA, 2023, pp. 276–277, doi: 10.1109/QCE57702.2023.10240.

[16] D. Konar, V. Aggarwal, A. D. Sarma, *et al.*, "Deep Spiking Quantum Neural Network for Noisy Image Classification," *2023 Int. Joint Conference on Neur. Net. (IJCNN)*, Gold Coast, Australia, 2023, pp. 1–10, doi: 10.1109/IJCNN54540.2023.10191509.

[17] D. Konar, D. Peddyreddy, V. Aggarwal, *et al.*, "Tensor Ring Optimized Quantum-Enhanced Tensor Neural Networks," *arXiv*, 2023, pp. 1–15, doi: https://doi.org/10.48550/arXiv.2310.01515.

[18] C. Roman-Vicharra, and J.J. Cai, "Quantum gene regulatory networks," *npj Quantum Inf.*, vol. 9, no. 1, pp. 67, 2023, doi: https://doi.org/10.1038/s41534-023-00740-6.

[19] D. Sarnataro, "Attempt to untangle the prion-like misfolding mechanism for neurodegenerative diseases", *Int. Jour. of Molecular Sciences*, vol. 19, no. 10, pp. 3081, 2018, doi: https://doi.org/10.3390/ijms19103081.

[20] M. Lambert, A. Barlow, B. Chromy, *et al.*, "Diffusible, nonfibrillar ligands derived from $A\beta$ are potent central nervous system neurotoxins", *Proc. of the Nat. Acad. of Sc.*, vol. 95, no. 11, p. 6448–6453, 1998, doi: https://doi.org/10.1073/pnas.95.11.6448.

[21] M. C. Caro, H. Y. Huang, M. Cerezo, *et al.*, "Generalization in quantum machine learning from few training data," *Nat Commun.*, vol. 13, no. 4919, 2022, doi: https://doi.org/10.1038/s41467-022-32550-3

[22] V. Bottero, D. Powers, A. Yalamanchi, *et al.*, "Key Disease Mechanisms Linked to Alzheimer's Disease in the Entorhinal Cortex," *Int. J. of Mol. Sc.*, vol. 22, no. 8, 2021, doi: 10.3390/ijms22083915.

[23] Y. Zhang, R. Thompson, and H. Zhang, "APP Processing in Alzheimer's Disease," *Molecular Brain*, vol. 4, no. 3, 2011, doi: 10.1186/1756-6606-4-3.

[24] T. C. W. Julia, A. M. and Goate, "Genetics of β-Amyloid Precursor Protein in Alzheimer's Disease," *Cold Spring Harbor Perspectives in Medicine*, vol. 7, no. 6, 2017, doi: 10.1101/cshperspect.a024539.

[25] Y. Huang and L. Mucke, "Alzheimer mechanisms and therapeutic strategies", *Cell*, vol. 148, no. 6, p. 1204–1222, 2012, doi: https://doi.org/10.1016/j.cell.2012.02.040.

[26] R. Pluta, M. Ulamek-Koziol, S. Januszewski, *et al.*, "Shared genomic and proteomic contribution of amyloid and tau protein characteristic of Alzheimer's disease to brain ischemia", *Int. Journal of Molecular Sc.*, vol. 21, no. 9, pp. 3186, 2020, doi: https://doi.org/10.3390/ijms21093186.

[27] E. Razani, A. Pourbagheri-Sigaroodi, A. Safaroghli-Azar, *et al.*, "PLD3 affects axonal spheroids and network defects in Alzheimer's disease," *Nature*, vol. 612, no. 7939, pp. 328–337, 2022. doi: https://doi.org/10.1038/s41586-022-05491-6.

[28] E. Barbero-Camps, V. Roca-Agujetas, I. Bartolessis, *et al.*, "Cholesterol impairs autophagy-mediated clearance of amyloid beta while promoting its secretion", *Autophagy*, vol. 14, no. 7, pp. 1129–1154, 2018, doi: https://doi.org/10.1080/15548627.2018.1438807.

[29] X. Yue, Y. Kong, Y. Zhang, et al., "srebf2–stard4 axis confers sorafenib resistance in hepatocellular carcinoma by regulating mitochondrial cholesterol homeostasis", *Cancer Science*, vol. 114, no. 2, pp. 477–489, 2022. doi: https://doi.org/10.1111/cas.15449.

[30] A. Weintraub, C. Li, A. Zamudio, et al., "YY1 is a structural regulator of enhancer-promoter loops", *Cell*, vol. 171, no. 7, p. 1573–1588, 2017. doi: https://doi.org/10.1016/j.cell.2017.11.008.

[31] S. Cunnane, E. Trushina, C. Morland, *et al.*, "Brain energy rescue: an emerging therapeutic concept for neurodegenerative disorders of ageing", *Nature Reviews Drug Discovery*, vol. 19, no. 9, pp. 609–633, 2020, doi: https://doi.org/10.1038/s41573-020-0072-x.

[32] A. Gotoh, M. Hidaka, K. Hirose, *et al.*, "Gas7b (growth arrest specific protein 7b) regulates neuronal cell morphology by enhancing microtubule and actin filament assembly," *The Journal of Biological Chemistry*, vol. 288, no. 48, pp. 34699–706, 2013, doi: 10.1093/jb/mvs038.

[33] Y. T. Hu, X. L. Chen, S. H. Huang, *et al.*, "Early growth response-1 regulates acetylcholinesterase and its relation with the course of Alzheimer's disease.," *Brain Pathology*, vol. 29, pages 502–512, 2019, doi: 10.1111/bpa.12688.

[34] M. Hutton, C. Lendon, P. Rizzu, *et al.*, "Association of missense and 5-splice-site mutations in tau with the inherited dementia FTDP-17", *Nature*, vol. 393, no. 6686, pp. 702–705, 1998, doi: https://doi.org/10.1038/31508.

[35] X. Qin, Y. Wang, and H. K. Paudel, "Inhibition of Early Growth Response 1 in the Hippocampus Alleviates Neuropathology and Improves Cognition in an Alzheimer Model with Plaques and Tangles.," *The American Journal of Pathology*, vol. 187, no. 8, pages 1828–1847, 2017, doi: 10.1016/j.ajpath.2017.04.018.

[36] Wei-Chun J. Hsu, N. C. Wildburger, S. J. Haidacher, *et al.*, "PPARgamma agonists rescue increased phosphorylation of FGF14 at S226 in the Tg2576 mouse model of Alzheimer's disease," *Experimental Neurology*, vol. 295, pp. 1–17, 2017, doi: https://doi.org/10.1016/j.expneurol.2017.05.005.

[37] Jessica Di Re, Paul A. Wadsworth, and Fernanda. Laezza "Intracellular Fibroblast Growth Factor 14: Emerging Risk Factor for Brain Disorders." *Front. in Cellular Neurosc.*, vol. 11, 2017, doi: https://doi.org/10.3389/fncel.2017.00103.

[38] L. Wang *et al.* "A method for the expression of fibroblast growth factor 14 and assessment of its neuroprotective effect in an Alzheimer's disease model." *Experimental Neurology*, vol. 9, no. 12, page 994, 2021, doi: 10.21037/atm-21-2492.

[39] J. Wang, J. T. Yu, and L. Tan, "PLD3 in Alzheimer's disease." *Molecular Neurobiology*, vol. 51, no. 2, 2015, pp. 480–486, doi: 10.1007/s12035-014-8779-5.

[40] P. Yuan, M. Zhang, L. Tong, *et al.*, "The PI3K/AKT signalling axis in Alzheimer's disease: a valuable target to stimulate or suppress?," *Cell stress & chaperones*, vol. 26, no. 6, pp. 871–887, 2021. doi: 10.1007/s12192-021-01231-3.

[41] H. Wu, Y. Kirita, E. Donnelly, *et al.*, "Advantages of single-nucleus over single-cell RNA sequencing of adult kidney: rare cell types and novel cell states revealed in fibrosis", *Journal of the American Society of Nephrology*, vol. 30, no. 1, p. 23–32, 2018, doi: https://doi.org/10.1681/asn.2018090912.

[42] D. Jovic, X. Liang, H. Zeng, *et al.* "Single-cell RNA sequencing technologies and applications: A brief overview," *Clinical and Translational Medicine*, vol. 12, no. 3, pp. 694, 2022, doi: 10.1002/ctm2.694.

[43] E. Rieffel, and W. Polak, "ACM Computing Surveys," *An introduction to quantum computing for non-physicists.*, vol. 12374, 2000, doi: https://doi.org/10.48550/arXiv.quant-ph/9809016.

[44] D. Konar, A. D. Sarma, S. Bhandary, *et al.*, "A shallow hybrid classical-quantum spiking feedforward neural network for noise-robust image classification," *Applied Soft Computing*, vol. 136, 2023, no. 110099, https://doi.org/10.1016/j.asoc.2023.110099.

[45] A. Nagahara, D. Merrill, G. Coppola, *et al.*, "Neuroprotective effects of brain-derived neurotrophic factor in rodent and primate models of Alzheimer's disease", *Nature Medicine*, vol. 15, no. 3, pp. 331–337, 2009, doi: https://doi.org/10.1038/nm.1912.